

Quinoxaline-based small molecules: synthesis and investigation on their optoelectronic properties

JIYONG DENG*, QIANG TAO, DONG YAN, XIANWEI HUANG, YUNFENG LIAO

School of Chemistry and Chemical Engineering, Hunan Institute of Engineering, Xiangtan, Hunan, China

Small molecules of ThQuTh, CzQuTh, CzQuCz and TPAQuCz were designed and synthesized, based on quinoxaline acceptor, and electron donating groups, i.e. alkyl-thiophene, carbazole and triphenylamine on both side chains and molecular backbones. Their thermal, optical and electrochemical properties were systematically compared and studied. The absorption spectra of the small molecules were strongly affected by the donor units attached to quinoxaline. Strong electron donating groups, such as carbazole on the molecular backbone would lower optical band gap, resulting in a wide absorption and the strong donor on the side chain would enhance the absorption intensity in short wavelength region. The highest occupied molecular orbital (HOMO) energy levels of the four molecules were up-shifted with increasing the electron donating properties of donor units. The bulk-heterojunction organic solar cells with a device structure of ITO/PEDOT:PSS/SMs:PC₆₁BM/LiF/Al were fabricated, in which the small molecules functioned as donors while PC₆₁BM as acceptor. Because the electron-donating ability of carbazole (Cz), triphenylamine (TPA) is higher than that of thiophene (Th), CzQuTh, CzQuCz and TPAQuCz show higher power conversion efficiency (PCE) than that of ThQuTh. Furthermore, being the strongest in absorption intensity and widest in absorption spectrum, TPAQuCz has the highest power conversion efficiency. Further improvement of the device efficiency by optimizing the device structure is currently under investigation.

Keywords: *quinoxaline; acceptor materials; optoelectronic properties; solar cells*

1. Introduction

The foreseeable exhaustion of fossil fuels stimulates the pursuit of renewable energy. Harvesting solar energy by photovoltaic means has attracted enormous attention. Bulk heterojunction organic solar cells (BHJ-OSCs) including polymer solar cells (PSCs) and small molecules solar cells (SMSs) were studied. With the use of polymer donors and fullerene acceptors, the power conversion efficiencies (PCEs) of PSCs were improved dramatically in the last decade [1–8], reaching the highest value of 11.7 % [9]. Nonetheless, there are disadvantages with PSCs, such as unreliable batch-to-batch performance, high purity demand of ingredients, and poor controllability of polymer molecular weight [10, 11]. In contrast, the use of small molecules (SMs) for the fabrication of BHJ-OSCs is favorable because of well-defined structures, which are mono-dispersive, simple

to synthesize and easy to purify. They are highly mobile and have no end-group contaminants. Consequently, the use of SMs as charge carriers for BHJ-OSCs fabrication enables reliable batch-to-batch performance [12–16]. The highest PCE achieved so far for solution-processed SMs-based BHJ-OSCs is 10.01 % [15], somewhat lower than that of PSCs [17].

For the improvement of power conversion efficiency in BHJ-OSCs applications, SMs with low band gap, broad and strong solar light absorption, and high charge-carrier mobility are desired [18, 19]. Various strategies were developed to generate SMs of this kind. A popular approach is to synthesize SMs with alternating donor D and acceptor A monomer units. Among the D-A materials, the star-shaped ones, large in structure and purposely decorated with electron-donating groups are known to be mono-dispersive and highly soluble in organic solvents [20, 21].

With low band gap and being efficient for electron injection and transport, benzo-quinoxaline

*E-mail: djiyong@yeah.net

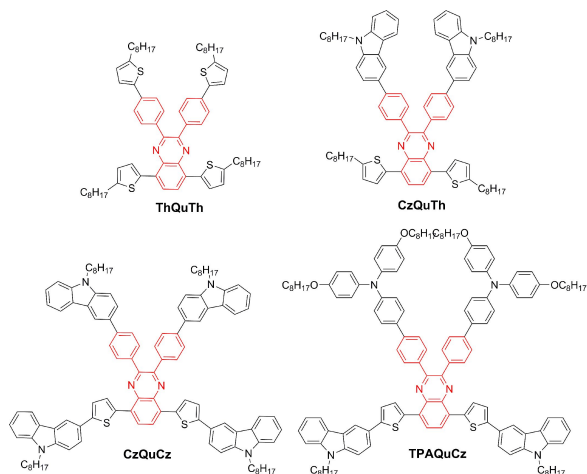


Fig. 1. Molecular structures of quinoxaline based SMs.

derivatives are used as acceptor units in polymer photovoltaic cells [22–25]. However, the quinoxaline moiety based small molecules have been reported rarely because of their low PCEs in solar cells. Additionally, the morphological investigations demonstrated that the low PCEs of quinoxaline moiety based small molecules were mainly due to the inappropriate phase segregation and limited light harvesting of the donor blends [26–28]. To further explore the potential of SMs as donor materials in organic solar cells, we report in this work, the design and synthesis of a series of star-shaped D-A molecules using benzo-quinoxaline as a core, by extending the π -conjugation, enhancing the solubility and intramolecular interactions (Fig. 1). With high electron affinity, benzo-quinoxaline is a good electron acceptor and the use of it can generate SMs with low band gaps. We attached thiophene (Th), carbazole (Cz) and triphenylamine (TPA) group to the core. The TPA and Cz groups are known to have good optical properties and hole transporting ability. Furthermore, the TPA unit is a three-dimensional propeller structure, and its presence promotes the amorphous nature and solution processability of the corresponding SMs. This kind of compounds has many innovative characteristics: (1) dipolarity due to charge transfer from electron-donating groups to the quinoxaline core and red shift of electronic absorption band [29]; (2) reduction of band gap due to internal charge transfer; and

(3) tuning of energy levels by adjusting the degree of intramolecular charge transfer through the introduction of different electron-donating moieties to the electron-withdrawing moiety.

In the present study, we investigated the photophysical, thermal, electrochemical and photovoltaic properties of the synthesized SMs. Furthermore, the nature of the BHJ-OSCs with the device structure of ITO/PEDOT:PSS/small molecule PC₆₀BM/LiF/Al was investigated. As envisaged, the benzo-quinoxaline core plays a positive role for the promotion of power conversion across the solar cells. What is more, the results demonstrate that by increasing the electron-donating ability of the D moiety, widening of absorption spectrum, improvement of thermal stability as well as enhanced photovoltaic performance can be achieved.

2. Experimental

2.1. Materials

All reagents and chemicals were purchased from commercial sources (Aldrich, Acros, TCI) and used without further purification unless stated otherwise. Tetrahydrofuran (THF) was distilled over sodium and benzophenone under an inert nitrogen atmosphere.

2.2. Instrumentation and measurements

Column chromatography was carried out with Merck silica gel (200 to 300 mesh). The NMR spectra were collected on a Bruker DPX 400 spectrometer using chloroform-d as a solvent and tetramethylsilane (TMS) as internal standard. Thermogravimetric analysis (TGA) was carried out using a Netzsch TG 209 analyzer at a heating rate of 10 °C min⁻¹ up to 600 °C. UV-Vis absorption spectra were recorded on a Perkin-Elmer Lambda 25 spectrometer. Cyclic voltammograms (CV) of the molecules were recorded on a CHI 660 electrochemical workstation at a scanning rate of 100 mV·s⁻¹. Their measurements were carried out at room temperature using a three-electrode setup with two platinum electrodes for both the working electrode and counter

electrode. Ag/AgCl was used as the reference electrode in an anhydrous acetonitrile solution with 0.1 M nitrogen-saturated tetrabutylammonium hexafluorophosphate (Bu_4NPF_6) calibrated with a ferrocene/ferrocenyl couple (Fc/Fc^+). The HOMO, LUMO energy levels (E_{HOMO} and E_{LUMO}) and electrochemical band gaps E_{g}^{ec} were calculated by the following equations:

$$E_{\text{HOMO}} = -(E_{\text{ox}} + 4.80) \text{ eV} \quad (1)$$

$$E_{\text{LUMO}} = -(E_{\text{HOMO}} + E_{\text{g}}^{\text{opt}}) \quad (2)$$

2.3. Solar cells fabrication and characterization

A traditional sandwich structure was used in the solar cell fabrication. The ITO/glass substrates were ultrasonic-cleaned by detergent, deionizer water, acetone and isopropanol for 15 min each in sequence. The resulting substrates were dried under a stream of nitrogen and subjected to the treatment of Ar/ O_2 plasma for 5 min. A layer of 30 nm of poly(3,4-ethylenedioxythiophene)-poly(styrenesulfonate) (PEDOT-PSS) film was spin-coated on ITO and then the substrates were baked at 140 °C for 10 min in a glove box. A blend solution of donor materials and [6,6]-phenyl-C-61-butyric acid methyl ester (PC_{61}BM) in chloroform were then spun cast onto the PEDOT:PSS layer. The substrates were dried under N_2 atmosphere at room temperature and then annealed at 150 °C for 15 min in a nitrogen-filled glove-box. Finally, 10 nm calcium and 100 nm aluminum films were deposited on the active layer under vacuum. The film thickness of the active layers was around 100 nm and active area was 0.1 cm^2 for each cell. The efficiency of a solar cell was evaluated under AM 1.5G irradiation of 100 $\text{mW}\cdot\text{cm}^{-2}$ intensity (Oriel 91160, 300 W) calibrated by a NREL-certified standard silicon cell. Current density-voltage (J-V) characteristics were examined in the dark using a computer-controlled Keithley 2602 source measurement unit. The cell was placed under monochromatic illumination (Oriel Cornerstone 260 1/4 m monochromator equipped with Oriel 70613NS QTH lamp) and

the incident light was calibrated with a monocrystalline silicon diode. All characterizations were performed under ambient conditions.

2.4. Synthesis

Compounds of 5-octyl-2-(tributylstannyl)-thiophene (1) [29], 4,7-bis(5-octylthiophen-2-yl)benzo[c][1,2,5] thiadiazole (2) [30], 4,7-bis(5-bromo-2-thienyl)-2,1,3-benzothiadiazole (4) [31], 1-(4-(9-octyl-9H-carbazol-3-yl)phenyl)-2-(4-(9-octyl-9H-carbazol-6-yl)phenyl)ethane-1,2-dione (8) [32], and N,N-bis((4-octyloxy)phenyl)-N-(4-(4,4,5,5-tetramethyl-1,3,2-dioxaborolan-2-yl)phenyl)benzenamine (9) [33] were synthesized according to the procedures in the literature. The synthetic routes are presented in Fig. 2.

5-octyl-2-(tributylstannyl)-thiophene (1)

A solution of n-BuLi (12 mL, 0.03 mol, in 2.5 M hexane) was added dropwise over a period of 1 h to a stirred solution of 2-n-octylthiophene (4.6 g, 0.023 mol) in 120 mL THF at -78 °C. The mixture was then stirred for another 2 h at -78 °C before chlorotributyltin (11 g, 0.03 mol) was added. The resulting mixture was stirred for 30 min and left under stirring at room temperature for 24 h. The reaction mixture was poured into 200 mL of water and extracted with ether. The combined organic phase was washed with brine, dried over anhydrous sodium sulfate (MgSO_4), and subjected to decompression evaporation to remove excess chlorotributyltin to afford the product as a yellow oil (9.2 g, yield: 94.2 %). ^1H NMR (400 MHz, CDCl_3 , TMS, δ_{ppm}): 7.00 (s, 1H), 6.92 (s, 1H), 2.87 (t, $J = 7.60$ Hz, 2H), 1.87 to 0.68 (m, 42H).

4,7-bis(5-octylthiophen-2-yl)benzo[c][1,2,5]thiadiazole (2)

A mixture of 4,7-dibromo-2,1,3-benzothiadiazole (1 g, 3.4 mmol), compound (1) (4.12 g, 6.8 mmol), $\text{Pd}(\text{PPh}_3)_4$ (0.10 g, 0.088 mmol) and 20 mL toluene was carefully degassed and charged with nitrogen. The mixture

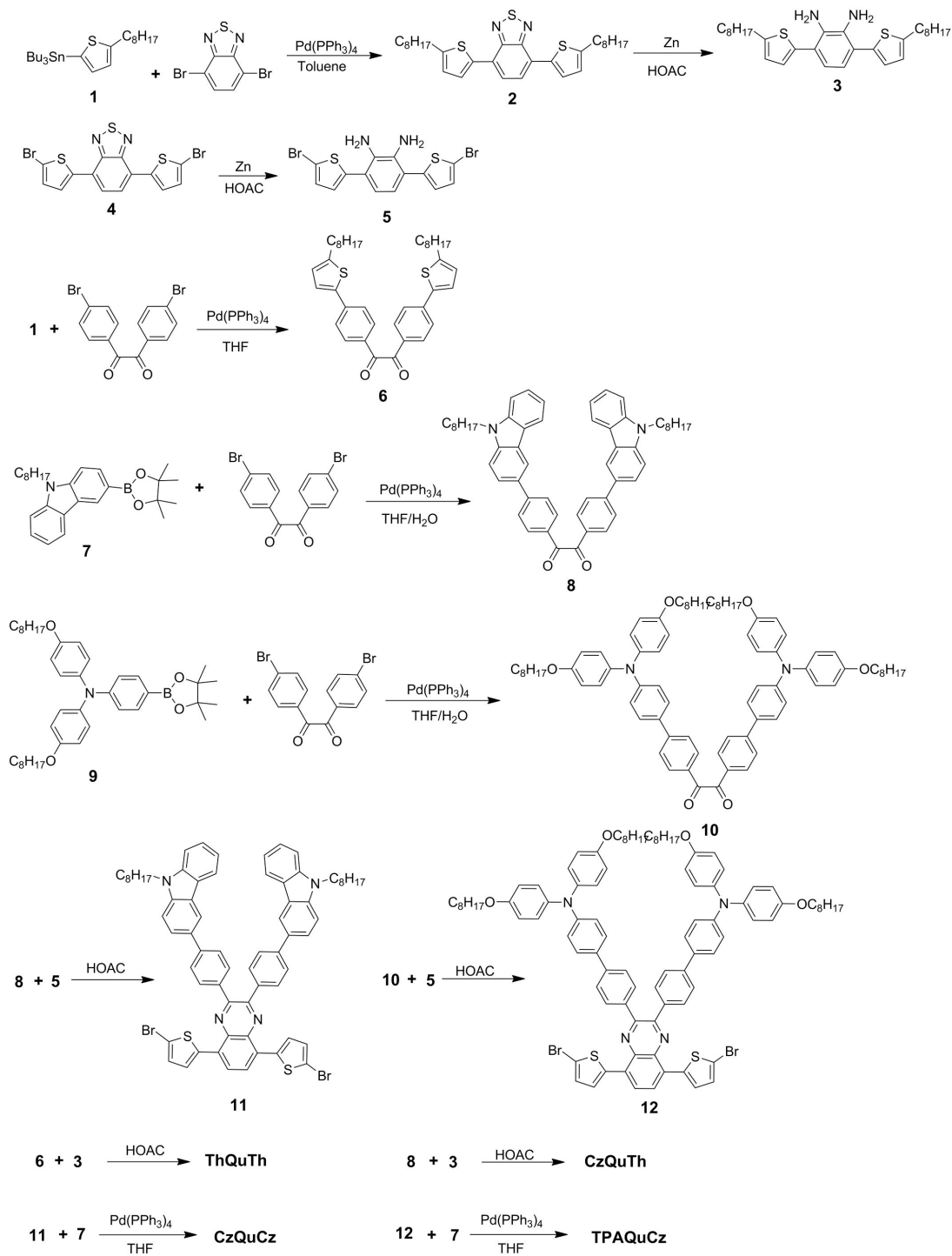


Fig. 2. The synthetic route for the four small molecules.

was then stirred for 30 min at 60 °C before it was heated to reflux for 24 h. After cooling to room temperature, the mixture was extracted

with chloroform. The combined organic phase was washed with brine, dried over anhydrous sodium sulfate (MgSO_4), and distilled over

the majority of solvent. The crude was purified by column chromatography using a mixture solvent of dichloromethane and petroleum ether (1:10) as eluent to afford the product as a red purple solid (0.71 g, yield: 39.9%). ^1H NMR (400 MHz, CDCl_3 , TMS, δ_{ppm}): 7.96 (d, $J = 4.0$ Hz, 2H), 7.31 (d, $J = 5.1$ Hz, 2H), 6.92 (d, $J = 3.2$ Hz, 2H), 2.93 (t, $J = 11.2$ Hz, 4H), 1.83 to 1.76 (m, 4H), 1.46 to 1.34 (m, 20H), 0.92 (d, $J = 13.6$ Hz, 6H).

3,6-bis(5-octylthiophen-2-yl)benzene-1,2-diamine (3)

To a solution of compound (2) (0.80 g, 1.52 mmol) in acetic acid (40 mL), zinc dust (1.23 g, 18.85 mmol) was added, and the mixture was stirred at 80 °C for 2 h and then subjected to filtration. The as-acquired liquid was basified with 2M NaOH and extracted three times with 100 mL of dichloromethane. The removal of solvent from the combined organic extracts using a rotary evaporator gave the product (0.62 g, yield: 84.3%) in the form of colorless oil.

3,6-bis(5-bromothiophen-2-yl)benzene-1,2-diamine (5)

According to a procedure similar to that of (3), compound (5) was obtained from (4) as a colorless solid with a yield of 83.1 %.

5,8-Bis(5-bromothiophen-2-yl)-2,3-bis(4-(9-octyl-9H-carbazol-3-yl)-phenyl)quinoxaline (11)

A suspension of compound (8) (0.45 g, 0.58 mmol) and compound (5) (0.30 g, 0.70 mmol) in acetic acid (18 mL) was heated to reflux for 24 h, during which a yellow precipitate was formed. After filtration, the residue was purified by column chromatography using a mixture of dichloromethane and petroleum ether (1:3) as eluent. The product (0.59 g, 87.3 % yield) was obtained as a yellow solid. ^1H NMR (400 MHz, CDCl_3 , TMS, δ_{ppm}): 8.55 (s, 2H), 8.29 (d, $J = 7.4$ Hz, 2H), 8.22 (s, 2H), 8.05 (d, $J = 8.2$ Hz, 4H), 7.95 (d, $J = 8.0$ Hz, 6H), 7.74 (d, $J = 3.7$ Hz,

2H), 7.60 (d, $J = 6.3$ Hz, 4H), 7.41 to 7.33 (m, 8H), 4.45 (t, $J = 6.9$ Hz, 4H), 2.03 to 2.00 (m, 4H), 1.52 to 1.37 (m, 20H), 0.97 (t, $J = 6.7$ Hz, 6H).

5,8-Bis(5-bromothiophen-2-yl)-2,3-bis(4-(N,N-bis((4-octyloxy)phenyl)N-benzenamine-3-yl)-phe-nyl)quinoxaline (12)

According to a procedure similar to that for the synthesis of compound (11), compound (12) was obtained after reacting compound (5) with compound (10) in 84.4 % yield as a deep yellow solid. ^1H NMR (400 MHz, CDCl_3 , TMS, δ_{ppm}): 7.90 (s, 2H), 7.76 (d, $J = 7.9$ Hz, 4H), 7.56 (d, $J = 7.9$ Hz, 4H), 7.45 (d, $J = 8.0$ Hz, 4H), 7.34 to 0.34 (m, 4H), 7.07 (d, $J = 7.6$ Hz, 4H), 6.98 (d, $J = 7.6$ Hz, 4H), 6.83 (d, $J = 8.4$ Hz, 8H), 6.72 (d, $J = 3.5$ Hz, 2H), 3.94 (t, $J = 5.8$ Hz, 8H), 2.03 to 1.66 (m, 8H), 1.52 to 1.17 (m, 40 H), 0.88 (d, $J = 6.7$ Hz, 12H).

Synthesis of ThQuTh

ThQuTh was prepared according to a procedure similar to that for the synthesis of compound (11), using compound (6) and compound (3) as raw materials, ThQuTh was a deep red solid with a yield of 80.7 %. ^1H NMR (400 MHz, CDCl_3 , TMS, δ_{ppm}): 8.17 (s, 2H), 7.92 (d, $J = 8.0$ Hz, 4H), 7.84 (d, $J = 3.1$ Hz, 2H), 7.71 (d, $J = 8.0$ Hz, 4H), 7.33 (d, $J = 2.9$ Hz, 2H), 6.98 (d, $J = 4.8$ Hz, 2H), 6.88 (s, 2H), 3.03 (t, $J = 7.3$ Hz, 4H), 2.95 (t, $J = 7.3$ Hz, 4H), 1.99 to 1.87 (m, 4H), 1.84 to 1.81 (m, 7.6 Hz, 8H), 1.58 to 1.41 (m, 40H), 1.01 (s, 12H). ^{13}C NMR (100 MHz, CDCl_3 , TMS, δ_{ppm}): 150.73, 149.15, 146.48, 141.03, 137.34, 137.19, 136.39, 135.34, 131.16, 130.99, 126.60, 126.47, 125.20, 125.08, 123.96, 123.33, 53.36, 31.93, 31.87, 30.33, 29.46, 29.35, 29.26, 29.21, 22.67, 14.09. MS (MSD, m/z): $\text{C}_{68}\text{H}_{86}\text{N}_2\text{S}_4$, 1059.68; found, 1059.475.

Synthesis of CzQuTh

CzQuTh was prepared according to a procedure similar to that for the synthesis of compound (11) using compound (8) with compound (3) as raw

materials; CzQuTh was a red solid with a yield of 87.4 %. ^1H NMR (400 MHz, CDCl_3 , TMS, δ_{ppm}): 8.41 (s, 2H), 8.16 (d, $J = 7.6$ Hz, 2H), 8.07 (s, 2H), 7.98 (d, $J = 7.9$ Hz, 4H), 7.86 to 7.68 (m, 8H), 7.48 to 7.41 (m, 6H), 7.33 to 7.15 (m, 2H), 6.88 (s, 2H), 4.32 (t, $J = 6.7$ Hz, 4H), 2.93 (t, $J = 7.3$ Hz, 4H), 1.89 to 1.88 (m, 4H), 1.82 to 1.79 (m, 4H), 1.47 to 1.24 (m, 40H), 0.86 (s, 12H). ^{13}C NMR (100 MHz, CDCl_3 , TMS, δ_{ppm}): 151.23, 149.15, 142.59, 140.95, 140.22, 137.22, 137.00, 136.50, 131.42, 131.08, 126.93, 126.55, 126.49, 125.85, 125.10, 124.02, 123.47, 123.04, 120.51, 119.00, 118.92, 109.00, 108.90, 43.26, 31.98, 31.84, 31.73, 30.34, 29.76, 29.72, 29.54, 29.42, 29.34, 29.33, 29.22, 29.05, 27.37, 22.73, 22.65, 14.16. MS (MSD, m/z): $\text{C}_{84}\text{H}_{96}\text{N}_4\text{S}_2$, 1225.82; found, 1226.656.

Synthesis of CzQuCz

A mixture of compound (11) (0.10 g, 0.09 mmol), compound (7) (0.09 g, 0.22 mmol), K_2CO_3 (11.87 mg, 0.09 mmol), THF/water (20 mL; 1:1 in volume), and $\text{Pd}(\text{PPh}_3)_4$ (2.98 mg, 0.0026 mmol) was carefully degassed and charged with nitrogen. The reaction mixture was heated to reflux for 24 h. After cooling to room temperature, the mixture was extracted with chloroform three times. The combined organic phase was separated, washed with brine, dried over MgSO_4 , and distilled over the majority of solvent. The crude was purified by column chromatography using a mixture solvent of dichloromethane and petroleum ether (1:1) as eluent to afford the product as a dull purple solid (0.71 g, yield: 39.9 %). ^1H NMR (400 MHz, CDCl_3 , TMS, δ_{ppm}): 8.44 (s, 4H), 8.11 (m, 8H), 7.99 to 7.72 (m, 10H), 7.47 to 7.41 (m, 12H), 7.24 to 7.19 (m, 6H), 7.08 (s, 2H), 4.31 (t, $J = 6.6$ Hz, 8H), 1.89 to 1.88 (m, 8H), 1.39 to 1.16 (m, 40H), 0.86 to 0.79 (m, 12H). ^{13}C NMR (100 MHz, CDCl_3 , TMS, δ_{ppm}): 140.91, 140.18, 131.41, 126.76, 125.75, 125.21, 123.45, 123.06, 120.68, 118.92, 109.02, 108.79, 53.47, 43.21, 31.85, 31.83, 29.75, 29.45, 29.41, 29.23, 29.05, 27.37, 27.34, 22.65, 22.64, 14.11. MS (MSD, m/z): $\text{C}_{108}\text{H}_{111}\text{N}_6\text{S}_2$, 1556.2; found, 1555.772.

Synthesis of TPAQuCz

TPAQuCz was prepared according to a procedure similar to that for the synthesis of CzQuCz using compound (12) and compound (7) as raw materials, TPAQuCz was purplish red solid with a yield of 68 %. ^1H NMR (400 MHz, CDCl_3 , TMS, δ_{ppm}): 8.57 (s, 2H), 8.26 to 8.23 (m, 4H), 8.10 (d, $J = 7.8$ Hz, 4H), 8.02 (s, 2H), 7.96 (d, $J = 8.2$ Hz, 2H), 7.80 (d, $J = 7.8$ Hz, 4H), 7.65 (d, $J = 8.2$ Hz, 4H), 7.55 (t, $J = 7.7$ Hz, 8H), 7.24 (t, $J = 9.0$ Hz, 10H), 7.14 (d, $J = 8.1$ Hz, 4H), 6.98 (d, $J = 8.4$ Hz, 8H), 4.30 (t, $J = 6.6$ Hz, 4H), 3.95 (t, $J = 6.2$ Hz, 8H), 1.91 to 1.75 (m, 12H), 1.47 (m, 60H), 0.86 (m, 18H). ^{13}C NMR (100 MHz, CDCl_3 , TMS, δ_{ppm}): 155.59, 148.55, 148.43, 140.88, 140.71, 139.96, 136.94, 136.76, 132.04, 131.32, 127.55, 126.70, 126.05, 125.95, 125.78, 123.64, 123.28, 122.94, 121.37, 120.76, 120.50, 119.07, 115.35, 108.95, 108.87, 53.46, 43.19, 31.90, 31.84, 29.46, 29.42, 29.32, 29.23, 29.05, 27.36, 26.28, 22.73, 22.65, 14.17, 14.12. MS (MSD, m/z): $\text{C}_{136}\text{H}_{154}\text{N}_6\text{O}_4\text{S}_2$, 2000.85; found, 2001.130.

3. Results and discussion

3.1. Thermal stability

The thermal properties of four SMs were evaluated with thermogravimetric analysis (TGA). The recorded TGA curves are shown in Fig. 3. The corresponding data are summarized in Table 1. Decomposition temperatures T_d at 5 % weight loss of ThQuTh, CzQuTh, CzQuCz and TPAQuCz are observed at 463, 479, 501, and 451 °C, respectively. The relatively high T_d indicates that all the small molecules have good thermal stability and they are suitable for the fabrication of devices [34].

3.2. Optical properties

The normalized UV-Vis absorption spectra of the four small molecules in diluted CHCl_3 solution are displayed in Fig. 4a, and the corresponding data are compiled in Table 1. All the compounds exhibit multiple absorption bands in the range of 250 nm to 650 nm. In the range of 280 nm to 400 nm, the high absorption intensity can be attributed to

Table 1. Thermal, optical and electrochemical properties of ThQuTh, CzQuTh, CzQuCz and TPAQuCz.

Compounds	T_d [°C]	Solution	Film	E_g^{opt} [eV] ^a	E_{HOMO} [eV]	E_{LUMO} [eV] ^b
		λ_{abs} [nm]	λ_{abs} [nm]			
ThQuTh	463	314, 345, 430	339, 489	2.09	-5.18	-3.09
CzQuTh	479	302, 418	358, 429	2.01	-5.02	-3.01
CzQuCz	501	298, 357, 517	367, 540	1.77	-4.97	-3.20
TPAQuCz	451	290, 360, 521	367, 548	1.82	-4.96	-3.13

^aBand gap estimated from optical absorption band edge of the film.

^b $E_{LUMO} = -(E_{HOMO} + E_g^{opt})$.

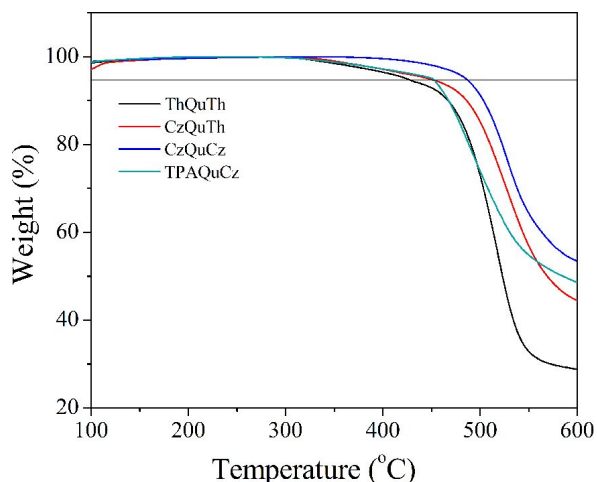


Fig. 3. TGA curves of ThQuTh, CzQuTh, CzQuCz and TPAQuCz.

$\pi \rightarrow \pi^*$ transition of molecular backbone, and the weaker broad band in the visible region (400 nm to 650 nm) to intramolecular charge transfer between the donor units and quinoxaline. The relative intensity of the former is significantly higher than that of the latter across the four molecules. There are variations probably caused by the donors attached to the quinoxaline core. Both CzQuCz and TPAQuCz exhibit extended absorption edges as compared ThQuTh and CzQuTh, showing that the electron-donating ability of TPA and Cz is stronger than that of Th. Consequently, the intramolecular charge transfer of CzQuCz and TPAQuCz is larger than that of ThQuTh and CzQuTh [34]. Moreover, TPAQuCz exhibits higher absorption intensity than CzQuCz, probably because the intramolecular charge transfer of TPA to quinoxaline core is stronger than that of Cz [35].

Fig. 4b shows the optical absorption spectra of ThQuTh, CzQuTh, CzQuCz and TPAQuCz in thin films. They show absorption slightly shifted to longer wavelength in comparison with their counterparts in solution. Such distinct bathochromic shift is because the intermolecular interaction in solid state is stronger than that in liquid state [29]. The absorption edge of the films is at ca. 591 nm, 616 nm, 700 nm, and 681 nm for ThQuTh, CzQuTh, CzQuCz and TPAQuCz, respectively, corresponding to band gaps of 2.09 eV, 2.01 eV, 1.77 eV, and 1.82 eV. It is apparent that the attachment of TPA and Cz with strong electron-donating ability to the quinoxaline core can significantly lower the band gap.

3.3. Electrochemical properties

Cyclic voltammetry was performed to investigate the electrochemical properties and to estimate the HOMO and LUMO energy levels of ThQuTh, CzQuTh, CzQuCz and TPAQuCz [36]. Fig. 5 shows the cyclic voltammograms of ThQuTh, CzQuTh, CzQuCz and TPAQuCz films in the positive potential range, illustrating the p-doping processes of the compounds. All the compounds exhibit an irreversible oxidation potential (E_{ox}) at approximately 0.78 eV, 0.62 eV, 0.57 eV and 0.56 V for ThQuTh, CzQuTh, CzQuCz and TPAQuCz, respectively (Table 1). However, no reduction of potentials (E_{red}) has been detected. Therefore, the HOMO energy levels (E_{HOMO}) have been calculated based on the empirical formula: $E_{HOMO} = -(E_{ox} + 4.80)$ eV [37]. The LUMO energy levels (E_{LUMO}) have to be estimated using the E_{HOMO} and optical band gap (E_g) values.

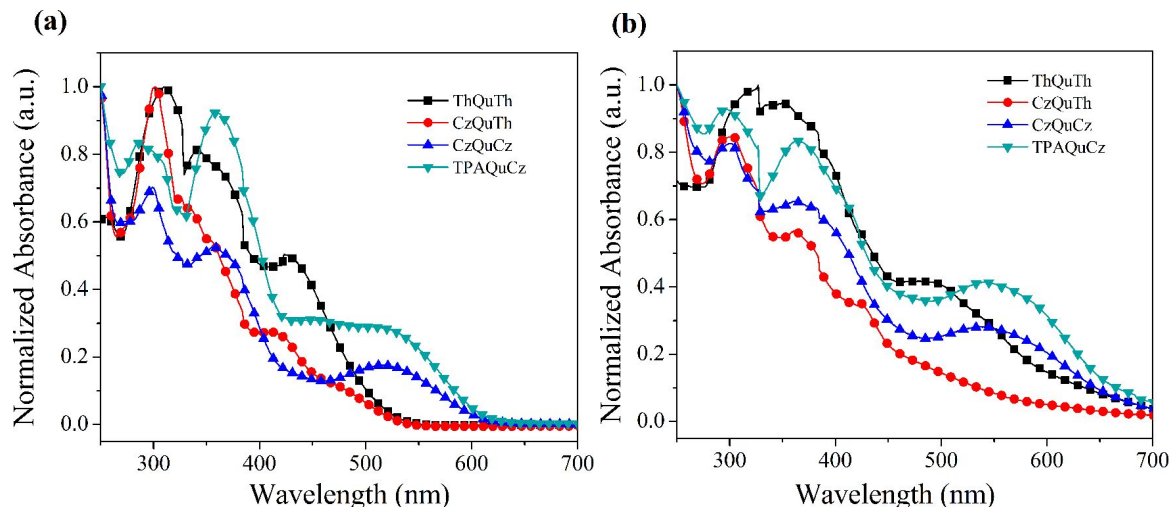


Fig. 4. UV-Vis spectra of ThQuTh, CzQuTh, CzQuCz and TPAQuCz (a) in chloroform; (b) in thin films.

In this aspect, E_g was estimated to be about 2.09 eV, 2.01 eV, 1.77 eV and 1.82 eV based on the UV-Vis absorption spectra of the corresponding films (Fig. 4b). The results of electrochemical measurements and calculated energy levels of the small molecules are listed in Table 1.

From Table 1, it is clear that the HOMO levels of ThQTh (-5.18 eV), CzQTh (-5.02 eV), CzQCz (-4.97 eV) and TPAQuCz (-4.96 eV) gradually increase, corresponding to the increase of electron-donating abilities of the donor units in these D-A type small molecules [34]. It can be seen that the LUMO levels of ThQuTh (-3.09 eV), CzQuTh (-3.01 eV), CzQuCz (-3.20 eV) and TPAQuCz (-3.13 eV) show a trend of gradually decreasing. It is apparent that the LUMO energy levels can be tuned by adjusting the electron-donating capacity of the moieties conjugated to quinoxaline. Furthermore, the relatively low LUMO energy levels of the four small molecules could be attributed the strong reduction capacity of the quinoxaline acceptor unit.

3.4. Photovoltaic performance

To investigate the photovoltaic properties of ThQuTh, CzQuTh, CzQuCz and TPAQuCz as an electron donor in BHJ-OSCs, photovoltaic devices were fabricated with a layer structure of ITO/PEDOT:PSS/small

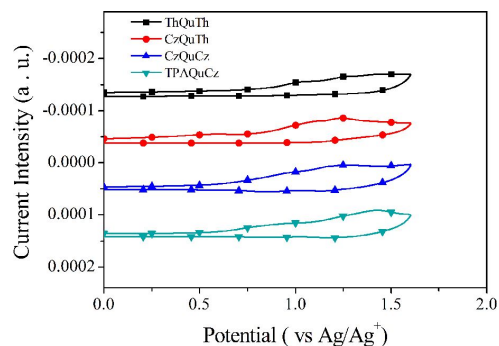


Fig. 5. CV curves of ThQuTh, CzQuTh, CzQuCz and TPAQuCz.

molecules:PC₆₁BM/LiF/Al. The J-V characteristics of the cells measured under the illumination of AM 1.5 G ($100 \text{ mW}\cdot\text{m}^{-2}$) from a solar simulator are shown in Fig. 6, and the photovoltaic performances of the devices are summarized in Table 2. It is shown that the PCEs rise from 0.05 % to 0.37 % for the devices that are based on ThQuTh, CzQuTh, CzQuCz and TPAQuCz. From Table 2, it is clear that the J_{sc} and FF of the ThQuTh-, CzQuTh-, CzQuCz- and TPAQuCz-based BHJ-OSCs gradually increase together with the increase of electron-donating ability of the D moieties. However, the J_{sc} of the TPAQuCz-based device is $1.91 \text{ mA}/\text{cm}^2$, which is lower than that of the CzQuCz-based device. The phenomenon may be attributed to the difference in charge transport

Table 2. Photovoltaic parameters of ThQuTh, CzQuTh, CzQuCz and TPAQuCz based solar cells.

SMs	D/A ratio	V_{oc} [V]	J_{sc}^a [$\text{mA}\cdot\text{cm}^{-2}$]	FF [%]	PCE [%]
ThQuTh	1:3	0.47	0.47	22.6	0.05
CzQuTh,	1:3	0.59	0.89	22.9	0.12
CzQuCz	1:3	0.47	2.24	23.7	0.25
TPAQuCz	1:3	0.68	1.91	28.0	0.37

abilities from the D units to the quinoxaline core. The V_{oc} is related to the difference between the LUMO energy level of the acceptor and the HOMO energy level of the donor within the active layer. Thus, the fact that the device based on CzQuTh:PC₆₁BM has higher V_{oc} (0.59 V) comparing with that based on ThQuTh:PC₆₀BM ($V_{oc} = 0.47$ V) could be explained by the HOMO energy level of CzQTh (-5.02 eV) as compared to that of ThQuTh (-5.18 eV). However, from Table 2, it is clear that despite CzQuCz has higher E_{HOMO} , the TPAQuCz:PC₆₁BM device has higher V_{oc} (0.68 V) than the CzQuCz:PC₆₁BM ($V_{oc} = 0.47$ V). The lower V_{oc} of the latter can be due to the relatively poor dispersibility of CzQuCz in the PC₆₁BM matrix.

Furthermore, the efficiency of power conversion of the TPAQuCz:PC₆₁BM device is the highest (0.37 %), showing a V_{oc} of 0.68 V, a J_{sc} of $1.91 \text{ mA}/\text{cm}^2$ and a FF of 0.28, higher than that of CzQuCz:PC₆₁BM. This could be due to the stronger absorption intensity of TPAQuCz in comparison with CzQuCz. Also, the efficiency for power conversion of the CzQuCz:PC₆₁BM device (0.25 %) is higher than that of CzQuTh:PC₆₁BM (0.12 %) and ThQuTh:PC₆₁BM (0.05 %). Clearly the gradual replacement of Cz, a strong donor, with Th, a weak donor, results in the decline of efficiency. Hence, the power conversion efficiency of this kind of BHJ-OSCs is dependent on the electron-donating ability as well as the absorption intensity of the SMSs.

4. Conclusions

Benzo-quinoxaline derivatives with low band gap are apt for electron injection and transport. The four small molecules of star shape

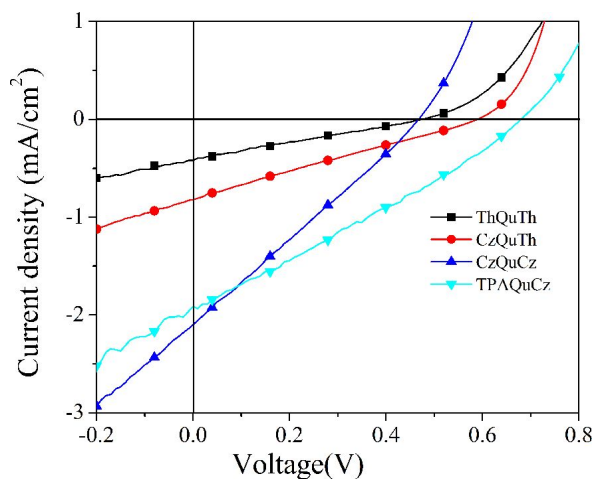


Fig. 6. J-V curves of ThQuTh, CzQuTh, CzQuCz and TPAQuCz based solar cells.

having electron-deficient benzo-quinoxaline core were synthesized and characterized. The films made of the SMs display morphology that indicates good dispersibility of the small molecules. Optical and electrochemical data reveal that the replacement of a weak donor Th with a strong donor Cz leads to an obvious increase of HOMO level and an even larger increase of LUMO level, resulting in band-gap contraction. The use of TPAQuCz instead of CzQuCz in BHJ-OSCs devices leads to oxidation potential similar to that in solution but results in higher efficiency of power conversion, plausibly due to the stronger absorption intensity of TPAQuCz. Also, the PCEs increase with the rise of electron-donating ability of the D units, indicates that the small molecules with a benzo-quinoxaline core can be modified for improved solar cell performance. With careful design, this class of SMs could be promising organic photovoltaic materials for the development of solar cells.

Acknowledgements

This work was supported by a Grant from the National Natural Science Foundation of China (Grant No. 21207034) and a Grant from the Natural Science Foundation of Hunan Province (Grant No. 2015JJ2042). The authors also express their thanks to Prof. C.T. Au for polishing the English writing of the paper.

References

- [1] JIN Y., CHEN Z., DONG S., ZHENG N., YING L., JIANG X.F., LIU F., HUANG F., CAO Y., *Adv. Mater.*, 28 (2016), 9811.
- [2] LEE J., SIN D.H., MOON B., SHIN J., KIM H.G., KIM M., CHO K., *Energ. Environ. Sci.*, 10 (2017), 247
- [3] RO H.W., DOWNING J.M., ENGMANN S., HERZING A.A., DELONGCHAMP D.M., RICHTER L.J., MUKHERJEE S., ADE H., ABDELSAMIE M., JAGADAMMA L.K., AMASSIAN A., LIU Y., YAN H., *Solar Cell. Energy Environ. Sci.*, 9 (2016), 2835
- [4] ZHANG B., LIANG J.F., HU L.W., PENG F., CHEN G.T., YANG W., *J Mater Sci.*, 16 (2015), 5609.
- [5] LIU Y., ZHAO J., LI Z., MU C., MA W., HU H., JIANG K., LIN H., ADE H., YAN H., *Nat. Commun.*, 5 (2014), 5293.
- [6] LI Y., YUE G.T., CHEN X.X., HE B.L., CHU L., CHEN H.Y., WU J.H., TANG Q.W., *J Mater Sci.*, 9 (2013), 3528.
- [7] ZHENG Z., ZHANG S., ZHANG J., QIN Y., LI W., YU R., WEI Z., HOU J., *Adv. Mater.*, 28 (2016), 5133.
- [8] QIAO F., LIU A.M., HU Z.Q., LIU Y.T., YU S.W., ZHOU Z.G., *J. Mater. Sci.*, 13 (2009), 3462.
- [9] ZHAO J., LI Y., YANG G., JIANG K., LIN H., ADE H., MA W., YAN H., *Nat. Energy*, 1 (2016), 15027.
- [10] ZHAO G.J., WU G.L., HE C., BAI F.Q., XI H.X., ZHANG H.X., LI Y.F., *J. Phys. Chem.*, 113 (2009), 2636.
- [11] WU G., ZHAO G., HE C., ZHANG J., HE Q., CHEN X., LI Y., *Sol. Energ. Mater. Sol. C.*, 93 (2009), 108.
- [12] LIN Y., LI Y., ZHAN X., *Chem. Soc. Rev.*, 41 (2012), 4245.
- [13] MISHRA A., BAUERLE P., *Ang. Chem.*, 51 (2012), 2020.
- [14] COUGHLIN J., HENSON Z., WELCH G., BAZAN G., *Chem. Res.*, 47 (2014), 257.
- [15] CHEN Y., WANG X., LONG G., *Acc. Chem. Res.*, 46 (2013), 2645.
- [16] WANG D., DING W., GENG Z., WANG L., GENG Y., SU Z., YU H., *Mater. Chem. Phys.*, 145 (2014), 387.
- [17] KAN B., LI M., ZHANG Q., LIU F., WAN X., WANG Y., NI W., LONG G., YANG X., FENG H., ZUO Y., ZHANG M., HUANG F., CAO Y., RUSSELL T.P., CHEN Y.A., *J. Am. Chem. Soc.*, 137 (2015), 3886.
- [18] SHI Q., CHENG P., LI Y., ZHAN X., *Adv. Energ. Mater.*, 2(2012), 63.
- [19] LINCKER F., DELBOSC N., BAILLY S., DE BETTIGNIES R., BILLON M., PRON A., DEMADRILLE R., *Adv. Funct. Mater.*, 18 (2008), 3444.
- [20] ZHANG J., YANG Y., HE C., HE Y., ZHAO G., LI Y., *Macromolecules*, 42 (2009), 7619.
- [21] YANG Y., ZHANG J., ZHOU Y., ZHAO G., HE C., LI Y., ANDERSSON M., INGANAS O., ZHANG F., *J. Phys. Chem. C*, 114 (2010), 3701.
- [22] ZHENG Z., AWARTANI O.M., GAUTAM B., LIU D., QIN Y., LI W., BATALLER A., GUNDOGDU K., ADE H., HOU J., *Adv. Mater.*, 5 (2016), 29.
- [23] FAN Q., XIAO M., LIU Y., SU W., GAO H., TAN H., WANG Y., LEI G., YANG R., ZHU W., *Polym. Chem.*, 6 (2015), 4290.
- [24] SU W., XIAO M., FAN Q., ZHONG J., CHEN J., DANG D., SHI J., XIONG W., DUAN X., TAN H., LIU Y., ZHU W., *Org. Electron.*, 17 (2015), 129.
- [25] FAN Q., LIU Y., XIAO M., SU W., GAO H., CHEN J., TAN H., WANG Y., YANG R., ZHU W., *J. Mater. Chem. C*, 3 (2015), 6240.
- [26] LEE D.-C., BROWNELL V.L., YAN L., YOU W., *ACS Appl. Mater. Interfaces*, 6 (2014), 15767.
- [27] CHANG D. W., KO S.-J., KIM J.Y., DAI L., BAEK J.-B., *Synth. Met.*, 162 (2012), 1169.
- [28] LI W., WANG D., WANG S., MA W., HEDSTROEM S., JAMES D. I., XU X., PERSSON P., FABIANO S., BERGGREN M., INGANAES O., HUANG F., WANG E., *ACS Appl. Mater. Inter.*, 7 (2015), 27106.
- [29] VELUSAMY M., HUANG J.H., HSU Y.C., CHOU H.H., HO K.C., WU P.L., CHANG W.H., LIN J.T., CHU C.W., *Org. Lett.*, 11 (2009), 4989.
- [30] HAGEMANN O., JØRGENSEN M., KREBS F.C., *J. Org. Chem.*, 71 (2006), 5546.
- [31] LIM B., BAEG K.J., JEONG H.G., JO J., KIM H., PARK J.W., NOH Y.Y., VAK D., PARK J.H., PARK J.W., KIM D.Y., *Adv. Mater.*, 21 (2009), 2808.
- [32] SVENSSON M., ZHANG F., VEENSTRA S.C., VERHEES W.J.H., HUMMELEN J.C., KROON J.M., INGANAS O., *Adv. Mater.*, 15 (2003), 988.
- [33] XU M.F., LI R.Z., POOTRAKULCHOTE N., SHI D., GUO J., YI Z.H., ZAKEERUDDIN S.M., GRATZEL M., WANG P., *J. Phys. Chem.*, 112 (2008), 19770. b) LIU M., WANG Y.F., ZHANG Z.Y., LI J.M., LIU Y., TAN H., NI M.J., LEI G.T., ZHU M.X., ZHU W.G., *J. Polym. Sci. Pol. Chem.*, 49 (2011), 3874.
- [34] LI Z., DONG Q., XU B., LI H., WEN S., PEI J., YAO S., LU H., LI P., TIAN W., *Sol. Energ. Mater. Sol. C.*, 95 (2011), 2272.
- [35] ZHANG W.F., NG G.M., TAM H.L., WONG M.S., ZHU F.S., *J. Poly. Sci. Part A: Poly. Chem.*, 49 (2011), 1865.
- [36] SO S., CHOI H., KIM C., CHO N., KO H.M., LEE J.K., KO J., *Sol. Energ. Mater. Sol. C*, 95 (2011), 3433.
- [37] LI Y.F., CAO Y., GAO J., WANG D.L., YU G., HEEGER A.J., *Synth. Met.*, 99 (1999), 243.

Received 2017-07-27

Accepted 2018-02-11